Crystallization Behavior and Crystal Structure of Poly(ethylene-*co*-trimethylene terephthalate)s

Xudong Chen,[1] Kun Yang,[1] Gong Hou,[1] Yujun Chen,[1] Yeping Dong,[1] Zhengfu Liao[1,2]

[1]*Institute of Polymer Science, School of Chemistry and Chemical Engineering, Sun Yat-Sen (Zhongshan) University, Guangzhou 510275, China*
[2]*Department of Chemistry, Guangxi Teachers Education University, Nanning 530001, China*

Received 14 September 2005; accepted 13 May 2006
DOI 10.1002/app.24993
Published online 23 May 2007 in Wiley InterScience (www.interscience.wiley.com).

ABSTRACT: A series of random copolymers were synthesized by the bulk polycondensation of dimethyl terephthalate with ethylene glycol (EG) and propane-1,3-diol (PDO) in various compositions. Their composition and thermal properties were investigated. The copolymers with 57.7 mol % or more PDO or 14.4 mol % or less PDO were crystallizable, but those with 36–46.2 mol % PDO were amorphous. The nonisothermal crystallization behavior was investigated with varying cooling rates by DSC. Poly(ethylene terephthalate) (PET) and poly(trimethylene terephthalate) (PTT) homopolymers have relatively lower activation energy than their copolymers. PET-rich copolymers (EG > 85.9%) exhibited PET crystal structure, and exhibited no PTT crystal structure; and PTT-rich copolymers (PDO > 41.7%) exhibited PTT crystal structure, and exhibited no PET crystal structure. © 2007 Wiley Periodicals, Inc. J Appl Polym Sci 105: 3069–3076, 2007

Key words: isothermal crystallization; poly(ethylene-*co*-trimethylene terephthalate); morphology; subsequent melting behavior; activation energy

INTRODUCTION

Poly(ethylene terephthalate) (PET) is a high-performance engineering plastic offering excellent thermal and mechanical properties, high chemical resistance, and low gas permeability. They are widely used as synthetic fibers, packaging films, bottles for beverages and food, recording and photographic tapes, and engineering plastic components.[1–3] However, PET still has some disadvantages, such as slow crystallization behaviors, which limit its applications. A lot of work has been done on its crystallization and melting behaviors have sought to overcome the crystalline characteristics of PET, including those of copolymerization.[4–8] In comparison to PET, poly(trimethylene terephthalate) (PTT) gained less attention previously because of the relatively high price of trimethylene glycol in the polymerization.[9] PTT was recently introduced commercially by Shell Chemicals under the trade name Corterra and its price is reduced. PTT is a semicrystalline polymer with outstanding elastic recovery, relatively low melt temperature, and rapid crystallization ability.[10–13] Because of the similarity in the chemical structure of these three linear aromatic polyesters, studies related to blends of PET and poly (butylene terephalate) (PBT),[14–16] and of PET and PTT,[17] and of PTT and PBT[18] are available in the open literatures. For these, PTT currently received great attention from both industry and academia to understand structure and property relationship as well as to find applications.[19–20]

In general, copolymerization affords a facile means of modifying the crystalline, morphology, melting point, glass transition temperature, etc. The copolyesters are of great commercial importance in the field of molding plastics and fibers. The structure–properties relationships of the copolyesters of a mixture of two glycols and a dicarboxylic acid are used in the synthesis of polymers with specific properties. The physical properties of copolyesters are related to their components, crystalline feature, and morphology. The chemical structure of PTT, which contains three methylene flexible segments per repeating unit, is similar to that of PET, which has two methylene moieties per repeating unit. Up to now, a few studies related to the subject of the crystallization behavior and crystal structure of the copolymers containing PET and PTT.

In this work, we have synthesized a series of copolyesters derived from dimethyl terephthalate, ethylene glycol (EG), and propane-1,3-diol (PDO) in varying proportions. This study investigated the crystallization kinetics, melting behaviors, and morphology of poly(ethylene-*co*-trimethylene terephthalate) (PETT)

Correspondence to: Dr. X. Chen (cescxd@zsu.edu.cn) or Z. Liao (Liaozhengfu@126.com).

Contract grant sponsor: Guangdong Province Natural Science Team Project of China; contract grant number: 20003038.

with DSC, FTIR, and X-ray diffraction (XRD). The objectives for this work are to asses the effect of even-numbered EG and odd-numbered PDO on the crystallization behaviors and morphology of PETT.

EXPERIMENTAL

Materials

Dimethyl terephthalate (DMT), obtained from Aldrich Chemical, was purified by recrystallization. Ethylene glycol (EG) and propane-1,3-diol (PDO) were distilled and used. Zinc acetate dehydrates and Sb_2O_3 were purchased from Aldrich Chemical, USA. All the chemicals were used as received without further purification.

Synthesis

A poly(ethylene-*co*-trimethylene terephthalate) (PETT) was synthesized by a three-step reaction sequence, including ester interchange, prepolycondensation, and polycondensation. The polymerization reactor was a 150-mL flask fitted with a special polymerization head containing N_2 inlet, a leak proof stirrer, and a condensation collector with an air-locked vacuum system. DMT, EG, and PDO were charged into the flask, followed by adding zinc acetate dehydrate as an ester interchange reaction catalyst. Then, the ester interchange reaction was conducted with stirring for 2.0–2.5 h at 220°C. During the reaction, methanol, as the by-product, was removed with a yield of 94% from the reaction mixture.

In the second step, the prepolycondensation reaction catalyst and a thermal stabilizer were added into the mixture. Then the bath temperature was gradually raised to 245°C, and the vacuum degree was raised to $\sim 1 \times 10^{-2}$ Torr, the prepolycondensation reaction was conducted with stirring until the methanol ceased and the pressure was reduced to 1 mmHg.

In the third step, the reaction temperature was raised to 270°C, the vacuum was raised to high vacuum degree, and the polycondensation reaction was conducted for 2.0–3.0 h. Then the bath was removed, and the polymer was dissolved in *o*-chloeophenol by reflux and precipitated in an excess quantity of ice-cold ethanol, filtered and dried in vacuum. The polymer was further purified by reprecipitation and employed for characterization.

In the same manner, a series of PETT copolyesters with various compositions were prepared with varying the compositions of DMT, EG, and PDO monomers.

Sample preparation

The samples of the copolyesters were hot-pressed into thin film $\sim$ 100 μm thick at temperatures $\sim$ 20–30°C above the melting temperatures (T_ms) and then were rapidly cooled to room temperature.

Characterization

Nuclear magnetic resonance

Compositions of the copolyesters synthesized were determined in a $CF_3COOD/CDCl_3$ (3 : 1 in volume)[21] using a proton nuclear magnetic resonance (^{1}H NMR) spectrometer (Varian INOVA 500 NB).

Intrinsic viscosity and molecular weight

Intrinsic viscosity was measured in CF_3COOH at (30 ± 0.1)°C using an Ubbelohde suspended level capillary viscometer.

Thermal analysis

Thermal characterization was performed under a dry nitrogen atmosphere using a differential scanning calorimeter (DSC) (Perkin–Elmer DSC-7). Furthermore, all specimens weighed 5.0–6.0 mg. In the DSC measurement, the polymer samples were preheated at 290°C for 20 min to remove their thermal history, and they were then quickly cooled to 0°C and heated to 290°C with a rate of 10°C/min. T_m was chosen as the temperature at the peak maximum of melting transition measured in the heating run and the heat of fusion (ΔH_f) was additionally estimated. T_g was chosen as the temperature at the middle point of glass transition obtained in the heating run. The heat of crystallization (ΔH_c) was obtained from the DSC thermogram.

Wide-angle X-ray diffraction

Linear θ/2θ X-ray intensity scans of these specimens were recorded with a D/MAX 2200VPC diffractometer in the reflection mode with Ni-filtered Cu Kα radiation.

Polarized optical microscope

Polarized optical microscopy (POM) was carried out with Olympus BH-2 optical microscope for observation of lamella changes in the spherulites.

RESULTS AND DISCUSSION

Synthesis

All the copolyesters were colorless and soluble in organic solvents such as *o*-chlorophenol, chloroform, *N*,*N*-dimethylacetamine, TFA, etc. For a series of PETT copolyesters synthesized, chemical compositions were determined by ^{1}H NMR spectroscopy. As

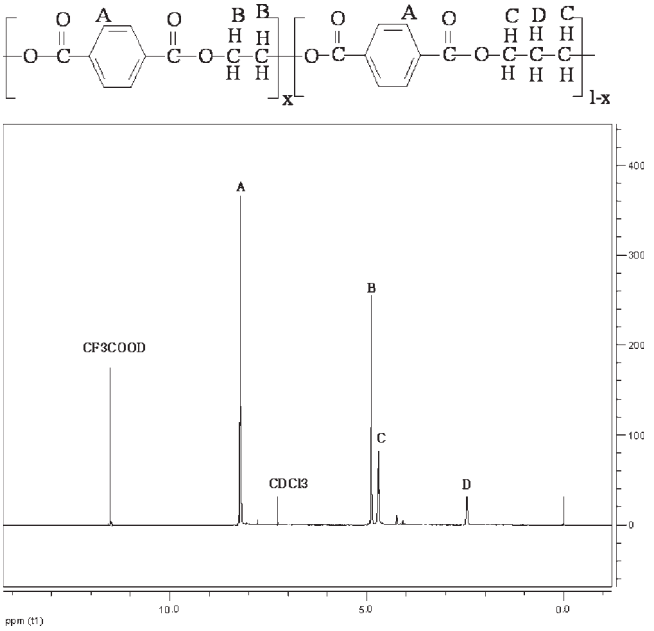

Figure 1 ^{1}H NMR spectra of PDO36 copolymer dissolved in a mixture solvent.

shown in Figure 1, the molar ratio of the 64% EG and 36% PDO units on the polymer backbone was estimated from integrations on their specific chemical shifts. All other samples are characterized in the same manner and the results are summarized in Table I. From Table I, we can find that the content of PDO unit incorporated into the copolymer is always larger than that fed in the bulk polymerization. This can be explained by two reasons: (1) PDO has one more methylene unit than EG. This methylene unit that chemically possesses an electron donor-ability leads to the more electronegativity of the oxygen atoms in PDO than that in EG, and the hydroxyl groups of PDO possesses a relatively strong nucleophile that can attack the carbonyl with DMT than EG in the ester exchange reaction, this leads to a relatively high content of PDO unit in the resultant copolymer. (2) The boiling point of PDO is higher than that of EG, the EG is easy to remove in the polymerization. All these will lead to a high content of PDO unit in the polyester copolymer.

For the copolyesters synthesized, the measured intrinsic viscosities ([η]s) were determined. The results are listed in Table I. The weight average molecular weight (M_w) was estimated from the measured intrinsic viscosities ([η]s) using the Mark–Hauwink–Sakurada equation with constants α and K, which were determined previously by Wallach[22] for PET homopolymer

$$[\eta] = 4.33 \times 10^{-4} M_w^{-0.68} \quad (1)$$

The results are listed in Table I. The estimated M_ws are in the range of 27,000–37,000, depending on the compositions. In fact, eq. (1) was found for PET homopolymer rather than PETT and copolymers, so that the M_w might be under- or overestimated. Overall, all the copolymers were however synthesized in reasonably high molecular weights.

Phase transition behavior

Figure 2 shows DSC thermograms of PET, PTT, and PETT copolyesters with various compositions, which were measured by heating with a rate 10.0°C/min. In particular, PET homopolymer shows a relatively weak glass transition. This might be due to its relatively high crystallinity. The copolyesters containing 58 mol % or more PDO, or 36 mol % or less PDO reveal two phase transitions: one appears over 30–80°C, which corresponds to the glass transition (T_g), and another over 180–260°C, which corresponds to the melting transition of crystals (T_m). However, the melting transitions of the copolymers appear very weakly, this is attributed to their relatively low crystallinities. In contrast, copolyesters with 36 mol % ≤ PDO unit ≤ 46

TABLE I
Composition, [η] of PETT Prepared with Various Feed Ratios of the Diol Monomer in the Polymerization

Polymer	Feed ratios of the diol monomer in the polymerization (EG/PDO)	Composition in the Polymer (EG/PDO)	Intrinsic viscosities ([η])	M_w
PET	100/0	100/0	0.530	34,000
PDO14	90/10	85.9/14.1	0.507	32,000
PDO36	80/20	64.0/36.0	0.523	34,000
PDO42	70/30	59.3/41.7	0.490	31,000
PDO46	60/40	53.8/46.2	0.532	35,000
PDO58	50/50	42.3/57.7	0.540	36,000
PDO70	40/60	30.1/69.7	0.496	31,000
PDO80	30/70	20.2/79.8	0.546	36,000
PDO87	20/80	12.9/87.1	0.553	37,000
PDO93	10/90	6.80/93.2	0.503	32,000
PTT	0/100	0/100	0.453	27,000

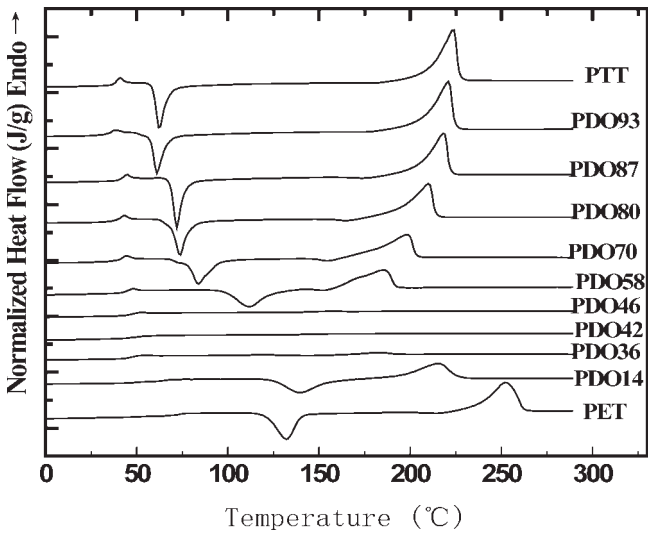

Figure 2 DSC cold crystallization and subsequent melting thermograms for quenched PETT copolymers with a heating rate of 10°C/min.

mol % show only one phase transition that corresponds to the glass transition; this indicates that these polymers are amorphous.

Glass transition temperature

Figure 2 shows the DSC cold crystallization and melting thermograms for quenching PTT, PET, and PETT copolymer samples recorded during heating at a heating rate of 10°C/min. All the PETT copolyesters exhibit single T_g, and the T_g decreases with increasing POD content. The depress of T_g is due to the chain flexibility enhanced by incorporation of PDO unit.

The analysis from Figure 2 showed that a single T_g value was located between those of the pure PTT and pure PET (i.e., $T_{g\mathrm{PTT}} = 37.5°\mathrm{C}$, $T_{g\mathrm{PET}} = 71.6°\mathrm{C}$), rather than two T_gs corresponding to possible blocks of ethylene terephthalate and trimethylene terephthalate. This evidence suggests that the copolymers synthesized with different comonomer ratios contained completely random comonomer sequences. The extract T_g can be seen in Figure 4.

The dependence of T_g value on the copolymer compositions for PETT copolymer is illustrated in Figure 3, the dotted line is the predicted T_g values for PETT copolymers according to the Fox equation.[23] Apparently, the Fox equation upperestimated the T_g value for the copolymers at all comonomer compositions. This may be due to the fact that the ΔC_p of these two comonomers was not of equal values, which evidently violates one of the assumptions used to attain the equation. As the Fox equation assumes random copolymer between the two comonomers, there are equal values of the ΔC_p in the glass-transition region between the homopolymers of the two comonomers (i.e., $\Delta C_{pA} = \Delta C_{pB}$).

Another well-known equation used to predict the composition-dependent behavior of T_g for a pair of block copolymers is the Gordon–Taylor equation,[24] which can be written as

$$T_g = \frac{W_A T_{gA} + kW_B T_{gB}}{W_A + kW_B} \tag{2}$$

where K is an adjustable parameter. The solid line shown in Figure 3 is the predicted composition-dependence of the T_g value for PETT copolymers according to the Gordon–Taylor equation, with the fitting k parameter being 0.195. On the basis of the predicted curve and the data shown in Figure 3, agreement between the observed T_g values and the prediction by the Gordon–Taylor equation was obtained at all copolymer compositions.

Crystallization behavior

From Figure 2, the cold crystallization (peak) temperature T_{cc} for PTT was observed; the observed T_{cc} values and cold crystallization heat (ΔH_{cc}) for PETT copolymers (taken from the thermograms shown in Fig. 2) were plotted against the copolymer composition in Figure 4. Obviously, a single and composition-dependent cold crystallization temperature was observed for most of the copolymers studied, except for the PDO36, PDO42, and PDO46 copolymers. The observed T_{cc} value for the copolymers was found to increase from $\sim$ 131.2°C of pure PTT to $\sim$ 139.6°C in the 14.1 PDO/85.9 EG copolymer and then level off to approach that of pure PTT. The copolymers with 57.7 mol % or more PDO or 14.4 mol % or less PDO were crystallizable, but those with 36–46.2 mol % PDO did

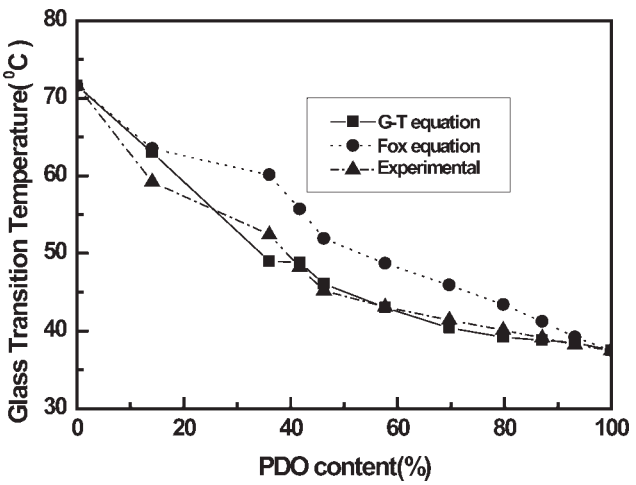

Figure 3 Observed glass transition temperature T_g for quenched PTT, PET, and PETT copolymer samples as a function of copolymer composition.

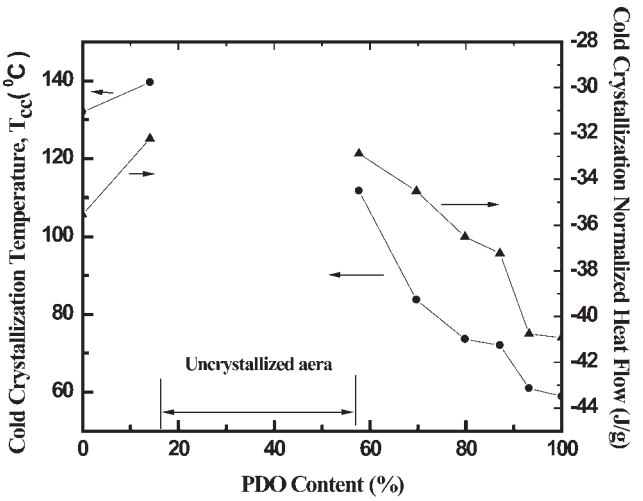

Figure 4 Observed T_{cc} and ΔH_{cc} for quenched PETT copolymers as a function of copolymer composition; (●) T_{cc}, (▲) ΔH_{cc}.

not have a T_{cc}, this indicated that those copolymers were amorphous. The result of cold crystallization heat (ΔH_{cc}) was similar to that of the cold crystallization temperature.

The observed T_m and melting heat (ΔH_m) values after cold crystallization for PETT copolymers (taken from the thermograms shown in Fig. 2) were plotted against the copolymer composition in Figure 5. Figure 5 shows the melt temperature T_m and the exothermic heat of melt (ΔH_m). PTT had a lower T_m than PET because of the presence of one more methylene unit in PTT than in PET, which increased the chain flexibility. The T_m and ΔH_m of PET are 252.3°C and 56.89 J/g, respectively; the T_m and ΔH_m of PETT containing 14.1 mol % PDO are 223.6°C and 33.66 J/g, respectively. When the content was in the range of 36–46.2 mol %, the copolymers were amorphous, the melt-temperature and the melt-exotherm were almost unobservable, and this suggested that crystallization was almost inhibited for these particular copolymers. When the content of PDO was more than 46.2 mol %, the T_m and ΔH_m of these copolymers increased with increasing content of PDO. These results may be due to these factors caused by the incorporated PDO or EG units as follows: (1) the incorporated component shortens the length of the crystallizable homopolymer block along the polymer chain. The shortened homopolymer crystallizable chain block may crystallize as relatively small, thin lamellar crystals. (2) The incorporated PDO or EG can lead to a reduction of the crystallinity, which is due to the decrease of the crystallizable chain block content. (3) The minor component PDO or EG incorporated disturbs the chain regularity that is necessary to make molecular ordering; the disturbed regularity may exert a negative influence on the crystal formation, and can lead to a reduction in both the lamellar crystal size and the crystallinity.

Figure 6 shows DSC melt-crystallization thermograms for PETT copolymers with a cooling rate of 10°C/min. According to Figure 7, the melt-crystallization temperature (T_{mc}) for PTT was observed around 179°C, whereas for PET it was observed around 202°C, this indicated that PTT was more crystallizable than PET. The observed T_{mc} values for PETT copolymers were plotted as a function of the copolymer composition in Figure 7. Similar to the case of cold crystallization and melt process, some copolymers did not have T_{mc}; this depended on their chemical compositions. The copolymers with 57.7 mol % or more PDO or 14.1 mol % or less PDO were crystallizable, but those with 36–46.2 mol % PDO were amorphous. T_{mc} and ΔH_{mc} of PET and PTT homopolymers were

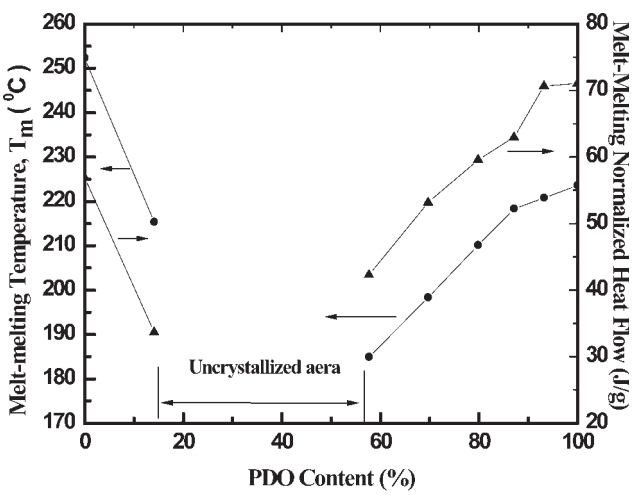

Figure 5 Observed T_m and ΔH_m for quenched PETT copolymers as a function of copolymer composition. (●) T_m, (▲) ΔH_m.

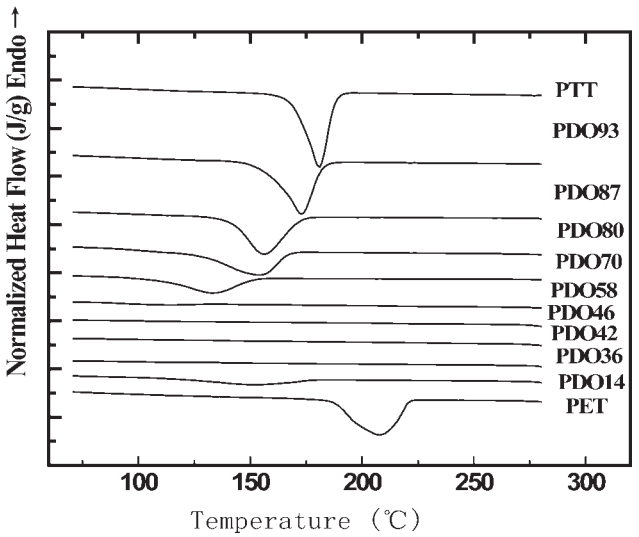

Figure 6 DSC melt-crystallization thermograms for PETT copolymers with a cooling rate of 10°C/min.

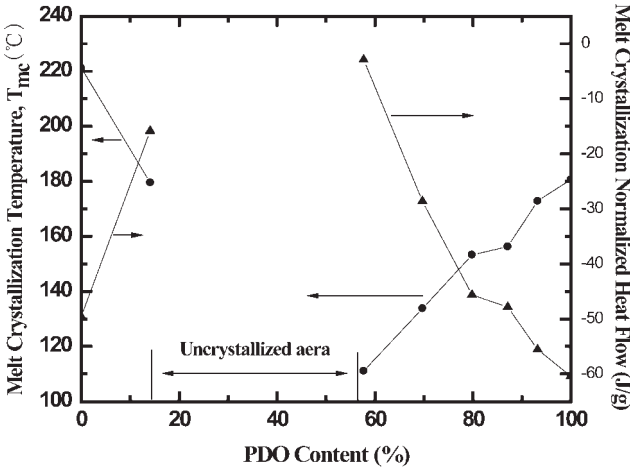

Figure 7 Observed T_{mc} and ΔH_{mc} for quenched PETT copolymers as a function of copolymer composition. (●) T_{mc}, (▲) ΔH_{mc}.

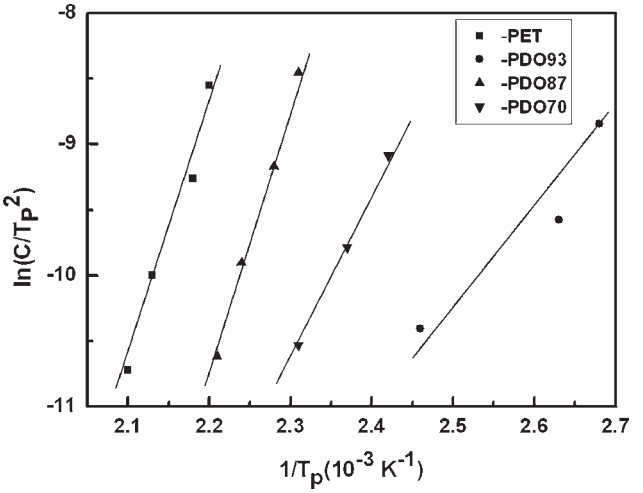

Figure 8 Kissinger plots of PET and PETT copolymers crystallized with various cooling rates.

reduced with the addition of PDO or EG as minor components. The results also suggested that an increase in the content of the minor component of PDO or EG retarded the crystallizability of the copolymers or, in other words, the crystallization ability of the major component in the copolymers decreased with an increasing content of the minor component.

Activation energy of nonisothermal crystallization

In a nonisothermal crystallization, the activation energy E_a can be derived from the variation of crystallization peak temperature T_p with the cooling rate by the Kissinger approach[25] as follows

$$\frac{d(\ln(C/T_p^2))}{d(1/T_p)} = -\frac{E_a}{R} \tag{3}$$

where R is the universal gas constant. The Kissinger plotting was performed for the T_ps and cooling rates Cs, which were measured for the PET, PTT, and their copolymers (shown in Fig. 8). The Kissinger plots exhibit a relatively good linearity. The crystallization activation energy was estimated from the slope in the plot. The E_a values of PET, PETT91, PETT46, PETT37, PETT28, PETT19, and PTT are −232.2, −178.6, −36.8, −43.1, −198.3, −226.9, and −257.4 kJ/mol, respectively. In the view of kinetics, the activation energy can be correlated to the crystallization rate. That is, the lower activation energy of crystallization drives the more rapid crystallization rate. From the activation energy value, we can also find that addition of the content of the minor component of PDO or EG retarded the crystallizability of PET or PTT, and the crystallization ability of the major component in the copolymers decreased with an increasing content of the minor component.

Crystal structure

The experimental results of DSC of PETT copolymers are different from those of PET-PBT copolymers; all PET-PBT copolymers are crystallizable.[26] There is only a methylene difference per repeating unit between PET and PTT, or PTT and PBT, but the difference between the properties of PETT and those of PET-PBT are large. So, we investigated the crystal structure of PETT copolymers using IR spectra and WAXD.

The IR spectra of PET, PTT, and PETT after annealing at 190°C for 12 h are shown in Figure 9. Since annealing is known to produce a significant increase in the degree of crystallinity, the bands showing increases and decreases in absorbance can be identified as crystalline and amorphous characteristics, respectively. According to the literature, the band of 1340 cm^{-1} is the crystalline characteristic band of the

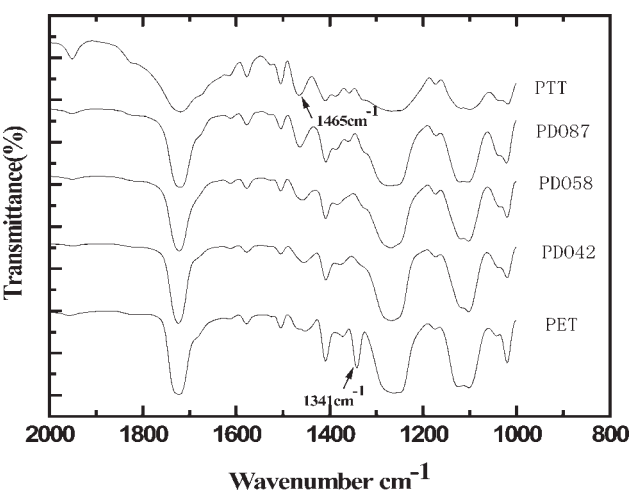

Figure 9 The IR spectra of PETT copolymers with different compositions.

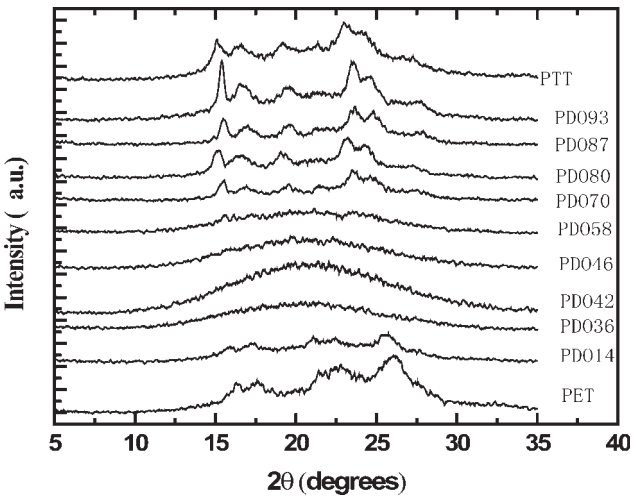

Figure 10 Wide-angle X-ray diffractograms of PETT copolymers with different compositions isothermally crystallized at 190°C for 30 min.

pure PET, the 1465 cm^{-1} band is associated with the scissoring mode of CH_2 in the crystalline phase, the most intense 1465 cm^{-1} peak is the crystalline reference peak of PTT.[27] From Figure 9, we can find that the shear vibration absorbance of CH_2 are 1453, 1455, 1458, 1464, and 1465 cm^{-1}, when the content of PDO is 0, 79.8, 57.7, 41.7, and 100%, respectively. The shear vibration absorbance peak of CH_2 increases with increasing PDO content, and the peak becomes sharp. At the same time, it can be found that the 1341 cm^{-1} band disappeared when the PDO content is up to 41.7%. So, we infer that PET-rich copolymers (EG $>$ 85.9%) exhibited PET crystal structure, and exhibited no PTT crystal structure; and PTT-rich copolymers (PDO $>$ 41.7%) exhibited PTT crystal structure, and exhibited no PET crystal structure.

To further confirm our inference, we investigated the crystal structure of PET, PTT, and their copolymers PETT by WAXD. The crystal structure of crystalline for PET, PTT, and their copolymers (after annealing at 190°C for 12 h) were observed with WAXD, the results of which are depicted in Figure 10. Some features can be noted: (1) the characteristic X-ray peaks for the pure PET were observed at the scattering angles (2θ) of about 16.3°, 17.7°, 21.4°, 22.8°, and 26.0°, corresponding to the reflection planes of $(0\bar{1}1)$, (010), $(\bar{1}11)$, $(1\bar{1}0)$, and (100), respectively [37]; the characteristic X-ray peaks for the PETT (EG/PDO = 85.9/14.1) were observed at the same scattering angles (2θ) of PET, this indicated that the characteristic X-ray peaks of the PETT (EG/PDO = 85.9/14.1) was as same as those of PET, and the crystal structure was that of PET. This indicated that the minor component block of PTT was too short to crystallize in the PET-rich copolymers. (2) In the case of PETT copolymers (EG/PDO in the range of 64/36–42.3/57.7), there are no characteristic X-ray diffraction peaks, this indicated that these copolymers are amorphous. (3) The characteristic X-ray peaks for the pure PTT were observed at the scattering angles (2θ) of about 15.4, 16.9, 19.5, 21.5, 24.4 and 27.4, corresponding to the reflection planes of (010), $(0\bar{1}2)$, (012), $(10\bar{2})$, (102), $(1\bar{1}3)$, and $(10\bar{4})$, respectively.[29] In the case of PETT copolymers (EG/PDO in the range of 30.1/69.9–0/100), the PETT copolymers have the same characteristic X-ray peaks with the pure PTT, this indicated that PTT-rich copolymers can only obtain the pure PTT crystal structure, there is no cocrystal. However, for the PET-PBT copolymers, the PBT and PTT components in the copolymers formed their own crystals.[30,31] This may indicate that the PETT copolymers shows the miscibility of PET and PTT segments in all of the amorphous and crystallized phase, but the PET-PBT copolymers shows the miscibility of PET and PBT segments in the amorphous phase and they crystallized separately according to its own cell. The explanation for this result is not yet available, and it should be a subject for further investigation.

Crystalline spherulitic morphology of PET, PTT, and their copolymer samples were recorded using polarized light optical microscopy (PLOM) with a

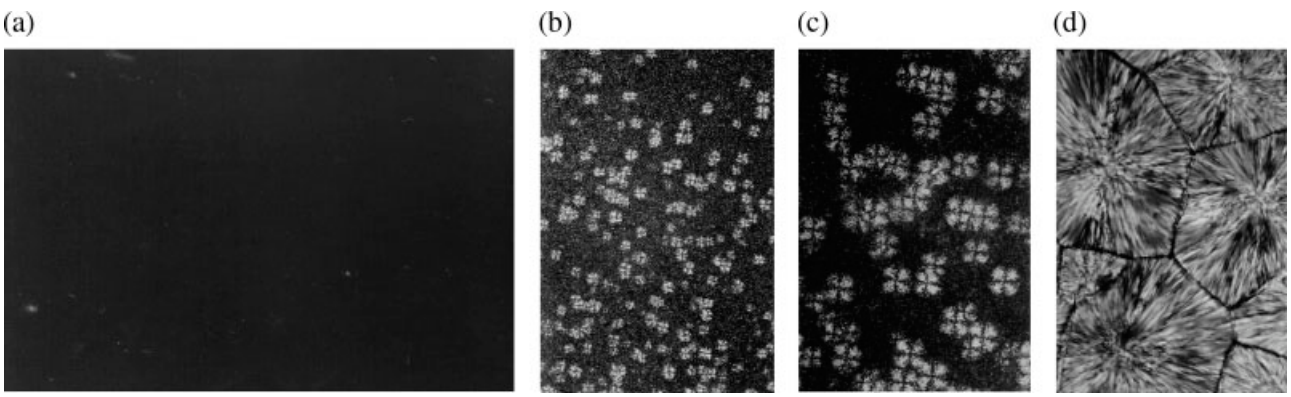

Figure 11 PLM photos of PETT copolymers with different compositions melt-crystallized at 190°C.

heating stage. Figure 11 shows the crystalline morphology in PLOM photos for PET, PTT, and their copolymers isothermally crystallized for 30 min at 190°C. The PTT and PTT-rich polymers show ring spherulites with the alternating yellow and white ring bands, and they also exhibit a pattern of a Maltese-cross in the spherulites. In addition, the spherulites apparently became coarser with increasing content of PDO. The yellow and white rings may not be of the conventional patterns because they are not of black and white contrasts as those reported in the literature.[32,33] For the yellow-white rings, the proper interpretation is still lacking. However, the POM images of PET and PET-rich polymer differed from those observed for the PTT and PTT-rich polymer, and the grown spherulite showed a dim Maltese cross, and the spherulite size decreases and the spherulite amount increases with adding PDO. However, those PETT copolymers (EG/PDO = 64/36, 59.3/41.7, 53.8/46.2, 42.3/57.7) were amorphous, so their POM images showed no spherulites.

CONCLUSIONS

All the PETT copolyesters exhibit single T_g. The T_g decreases with increasing POD content. It is due to the chain flexibility enhanced by incorporation of PDO unit.

The copolymers with 57.7 mol % or more PDO or 14.4 mol % or less PDO were crystallizable, but those with 36–46.2 mol % PDO did not have a T_{cc}, this indicated that those copolymers were amorphous. T_{mc} and ΔH_{mc} of PET and PTT homopolymers were reduced with the addition of PDO or EG as minor components. The results suggested that an increase in the content of the minor component of PDO or EG retarded the crystallizability of the copolymers or, in other words, the crystallization ability of the major component in the copolymers decreased with an increasing content of the minor component.

The nonisothermal crystallization behavior was investigated with varying cooling rate by DSC. The activation energy in the crystallization was estimated, PET and PTT homopolymers have relatively lower activation energy than their copolymers. The thermograms for PET and PETT (14 mol % PDO) samples exhibited single melting endothermic peaks, the melting behavior of PTT and PTT-rich copolymers exhibited the usually observed melting-crystallization-remelting phenomenon.

PET-rich copolymers (EG > 85.9%) exhibited PET crystal structure, and exhibited no PTT crystal structure; and PTT-rich copolymers (PDO > 41.7%) exhibited PTT crystal structure, and exhibited no PET crystal structure.

References

1. Brozenic, N. J. Modern Plastic Encyclopedia; McGraw-Hill: New York, 1986.
2. Ainsworth, S. A. Chemical and Engineering News, April 18, 1994; p 11.
3. Lee, S. W.; Lee, B.; Ree, M. Macromol Chem Phys 2000, 201, 451.
4. Holsworth, P. S.; Tumer-Jones, A. P. S. Polymer 1971, 12, 195.
5. Medelin-Rodriguez, F. J.; Phillips, P. J.; Lin, J. S.; Campos, R. J. J Polym Sci Part B: Polym Phys 1997, 35, 1757.
6. Xanthos, M.; Baltzis, B. C.; Hsu, P. P. J Appl Polym Sci 1997, 64, 1423.
7. Wu, T. M.; Chang, C. C.; Yu, T. L. J Polym Sci Part B: Polym Phys 2000, 38, 2515.
8. Zhou, C.; Clough, S. B. Polym Eng Sci 1988, 28, 65.
9. Bulkin, B. J.; Lewin, M.; Kim, J. S. Macromolecules 1987, 20, 830.
10. Supaphol, P.; Apiwanthanakom, N. J Polym Sci Part B: Polym Phys 2004, 42, 4151.
11. Apiwanthanakom, N.; Supaphol, P.; Nithitanakul, M. Polym Test 2004, 23, 817.
12. Xu, Y.; Ye, S. R.; Bian, J.; Qian, J. W. J Mater Sci 2004, 39, 5551.
13. Chung, W. T.; Yeh, W. J.; Hong, P. D. J Appl Polym Sci 2002, 83, 2426.
14. Lee, S. S.; Kim, J.; Park, M.; Lim, S.; Chul, R. C. J Polym Sci Part B: Polym Phys 2001, 39, 2589.
15. Avramova, N. Polymer 1995, 36, 801.
16. Yu, Y.; Choi, K. J. Polym Eng Sci 1997, 37, 91.
17. Supaphol, P.; Dangseeyun, N.; Thanomkiat, P.; Nithitanakul, M. J Polym Sci Part B: Polym Phys 2004, 42, 676.
18. Dangseeyun, N.; Supaphol, P.; Nithitanakul, M.; Polym Test 2004, 23, 187.
19. Lee, H. S.; Park, S. C.; Kim, Y. H. Macromolecules 2000, 33, 7994.
20. Kim, J. S.; Lewin, M.; Bulkin, B. J.; Hall, I. H. J Polym Sci Polym Part B: Polym Phys 1986, 24, 1783.
21. Pasquarelli, O. Presented at the SPE Seventh International Conference on High Performance Plastics Containers, New York, April 15–18, 1986.
22. Wallach, M. L. Makromol Chem 1967, 19, 103.
23. Fox, T. G. Bull Am Phys Soc 1956, 1, 123.
24. Gordon, M.; Taylor, J. S. J Appl Chem 1952, 2, 493.
25. Kissinger, H. E. J Res Natl Bur Stds 1956, 57, 217.
26. Misra, A.; Garg S. N. J Polym Sci Part B: Polym Phys 1986, 24, 983.
27. Kim, K. J.; Bae, J. H; Kim, Y. H. Polymer 2001, 42, 1023.
28. Wang, Z. G.; Hsiao, B. S.; Fu, B. X.; Lui, L.; Yeh, F.; Sauer, B. B.; Chang, H.; Schultz, J. M. Polymer 2000, 41, 1791.
29. Wang, B.; Li, Y. C.; Hanzlicek, J.; Cheng, S. Z. D.; Gail, P. H.; Grebowica, J.; Ho, R. M. Polymer 2001, 42, 7171.
30. Liu, Y. X.; Tong, Y. H.; Huang, Y. Q.; Li, Z. M. Polym Mater Sci Eng 1996, 12, 29.
31. Staumbaugh, B.; Koenig, J. L.; Lando, J. B. J Polym Sci Polym Lett Ed 1977, 15, 299.
32. Wang, Z.; An, L.; Jiang, W.; Jiang, B.; Wang, X. J. J Polym Sci Part B: Polym Phys 1999, 37, 2682.
33. Keith, H. D.; Padden, F. J., Jr. Macromolecules 1996, 29, 7776.